JOURNAL OF SPACECRAFT AND ROCKETS
Vol. 33, No. 5, September–October 1996

Mars Pathfinder Atmospheric Entry: Trajectory Design and Dispersion Analysis

David A. Spencer*
Jet Propulsion Laboratory, California Institute of Technology, Pasadena, California 91109
and
Robert D. Braun†
NASA Langley Research Center, Hampton, Virginia 23665

The Mars Pathfinder spacecraft will enter the Martian atmosphere directly from the interplanetary trajectory, with a velocity of up to 7.35 km/s. The definition of the nominal entry trajectory and the accurate determination of potential trajectory dispersions are necessary for the design of the Pathfinder entry, descent, and landing system. Monte Carlo numerical simulations have been developed to quantify the range of possible entry trajectories and attitude profiles. The entry trajectory requirements and constraints are discussed, and the design approach and uncertainties used in the Monte Carlo analysis are described. Three-degree-of-freedom and six-degree-of-freedom trajectory results are compared. The Monte Carlo analysis shows that the Mars Pathfinder parachute will be deployed within the required ranges of dynamic pressure, Mach number, and altitude, over a 3σ range of trajectories. The Pathfinder 3σ landing ellipse is shown to be roughly 50 × 300 km.

Nomenclature

$\boldsymbol{B}\cdot\boldsymbol{R}$	= component of the B-plane miss vector along the $\boldsymbol{R}$ axis, km
$\boldsymbol{B}\cdot\boldsymbol{T}$	= component of the B-plane miss vector along the $\boldsymbol{T}$ axis, km
C_3	= arrival energy, km^2/s^2
J_2	= second zonal harmonic coefficient in Mars gravitational potential
r	= radius from center of Mars to spacecraft center of mass, km
$\boldsymbol{S}\cdot\boldsymbol{R}$	= component of the angle between the estimated $\boldsymbol{S}$ direction and the nominal $\boldsymbol{S}$ direction, along the nominal B-plane $\boldsymbol{R}$ axis, rad
$\boldsymbol{S}\cdot\boldsymbol{T}$	= component of the angle between the estimated $\boldsymbol{S}$ direction and the nominal $\boldsymbol{S}$ direction, along the nominal B-plane $\boldsymbol{T}$ axis, rad
t_L	= linearized time of flight, s
α_T	= total angle of attack, deg
γ	= flight-path angle, deg
σ	= standard deviation

Introduction

THE primary objective of the Mars Pathfinder mission is to demonstrate a low-cost, reliable system for entering the Martian atmosphere and placing a lander safely on the surface of Mars. The entry, descent, and landing (EDL) system is designed to accommodate the range of off-nominal entry trajectories due to navigation errors and uncertainties in atmospheric density, entry body and parachute drag profiles, parachute deployment timing, and landing-site elevation. An overview of the EDL sequence of events is given. The design of the entry trajectory, along with the accurate determination of potential trajectory dispersions, is critical to the success of the Pathfinder mission. This paper discusses the requirements which led to the selection of the nominal trajectory. The nominal entry conditions and attitude profile are given. The parachute deployment algorithm which is implemented in the Monte Carlo simulations (and will also be used during actual mission operations) is described. For completeness, a backup method for deploying the parachute in the case of accelerometer failure is also discussed.

The Monte Carlo analysis approach is described. This analysis has been undertaken to assess the trajectory design margin in the presence of off-nominal conditions. Three-degree-of-freedom (DOF) and six-DOF Monte Carlo simulations have been developed to obtain statistical information on conditions at significant points during the Pathfinder descent. The three-DOF (translational) capability was used at the Jet Propulsion Laboratory for preliminary trajectory trade studies and computation of terminal descent (following parachute deployment) conditions. The six-DOF (translational and rotational) capability was developed at NASA Langley Research Center to give accurate trajectory and attitude information at critical times during the entry phase, prior to parachute deployment.[1] The results of the Monte Carlo simulations have directly influenced the design of the Pathfinder aeroshell thermal protection system[2] and have been used to design and test the parachute deployment algorithm. Through application of a Monte Carlo analysis, the size and orientation of the landing ellipse on the Mars surface has been determined.

EDL Overview

The Pathfinder spacecraft (a schematic is shown in Fig. 1) will enter the Martian atmosphere directly from the Earth-to-Mars

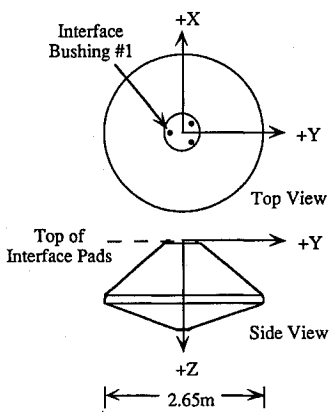

Fig. 1 Entry-body schematic and coordinate-system definition.

Presented as Paper 95-379 at the AAS/AIAA Astrodynamics Conference, Halifax, NS, Canada, Aug. 14–17, 1995; received Sept. 12, 1995; revision received Feb. 23, 1996; accepted for publication Feb. 26, 1996.

*Member, Technical Staff, Navigation and Flight Mechanics Section. Member AIAA.

†Aerospace Engineer, Space Systems and Concepts Division. Member AIAA.

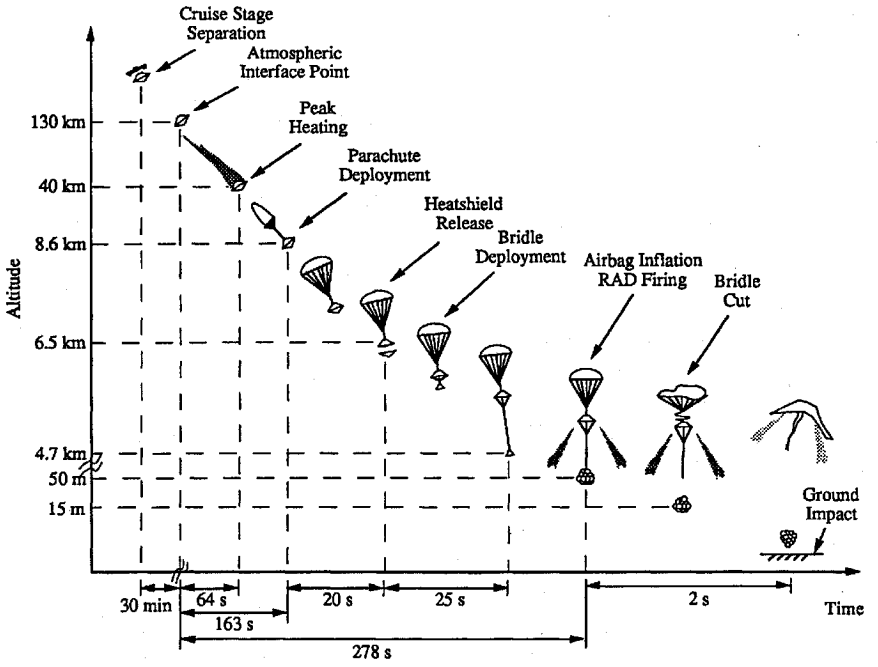

Fig. 2 EDL sequence of events.

interplanetary transfer trajectory, along a Mars-centered approach hyperbola.[3] Depending on the launch date, the entry vehicle will reach the atmospheric interface point (defined at a radius of 3522.2 km) with an inertial velocity of up to 7.35 km/s. The Pathfinder trajectory approach is in contrast to that of the Viking Landers; the Viking spacecraft entered orbit about Mars and imaged the planet surface for one month prior to entry, to find suitable landing sites. The Viking Landers entered the atmosphere with inertial velocities of roughly 4.5 km/s, and employed an active control system during the descent phase, concluding with soft landings on the Mars surface.[4] Pathfinder will not use active control during entry, but will rely upon a system of a parachute, solid rockets, and airbags to decelerate and buffer the spacecraft at landing.

The Pathfinder EDL sequence of events is shown in Fig. 2. Thirty minutes prior to atmospheric entry, the cruise stage will be jettisoned. The entry vehicle will enter the Mars atmosphere, reaching maximum stagnation-point heating and peak dynamic pressure during the initial 70 s of the entry phase. At 163 s past entry, a parachute will be deployed, followed by the release of the forebody heatshield 20 s later. The lander will be deployed below the backshell along a 20-m bridle. At an altitude of 1.5 km above ground level (AGL), a radar altimeter will acquire the ground. Altimeter data will be used by the flight software to inflate an airbag system and fire a set of three solid rockets (mounted on the backshell) at an altitude of 50 m AGL. At an altitude of 15 m, the bridle will be cut, and the lander will fall directly, buffered at ground impact by the airbag system. Sufficient impulse will remain in the solid rockets to carry the backshell and parachute to a safe distance away from the lander.

The Pathfinder target landing site is located at the outflow of a catastrophic flood system in the Ares Valles region[5] at 19.5°N, 32.8°W. It is expected that this region will contain samples of a wide variety of Martian surface materials.

Entry-Trajectory Requirements and Constraints

The Mars Pathfinder atmospheric entry trajectory is designed to fit within an envelope of derived requirements and physical constraints. The primary design parameter that is varied to keep the 3σ range of entry trajectories within the required envelope is the entry flight-path angle, defined as the angle between the inertial velocity vector and the local horizontal at the atmospheric interface point, negative toward the planet. The 3σ low (shallow) entry flight-path angle is bounded by the physical skipout angle constraint and the derived requirement on total integrated stagnation-point heating. The 3σ high (steep) entry flight-path angle is bounded by the physical stagnation-point pressure constraint of the aeroshell ablative material.

For the Pathfinder ballistic coefficient and entry velocity, the limiting flight-path angle for skipout from the Mars atmosphere is -11.2 deg (i.e., if the spacecraft inertial velocity vector is less than 11.2 deg below the local horizontal at the time of entry, skipout is predicted to occur). The Jet Propulsion Laboratory (JPL) Pathfinder Project Office has required that the entry trajectory be designed so that the 3σ shallow inertial flight-path angle at entry is at least 2 deg steeper than the skipout angle.

Arc-jet testing at NASA Ames Research Center has demonstrated that the aeroshell ablative material (SLA-561V) can maintain its physical integrity at stagnation-point pressures of 25.332 kPa (0.25 Earth atm) or less. At stagnation-point pressures greater than 25.332 kPa, surface spallation of the aeroshell ablative material can occur, effectively changing the aerodynamic characteristics of the aeroshell and creating uncertain heating conditions. The entry trajectory must be designed so that a statistical 3σ steep trajectory has a maximum stagnation-point pressure below the 25.332-kPa level. Peak heating rates were evaluated and included in the sizing of the thermal protection system; however, any requirement on the peak heating rate is superseded by the more constraining limit on the stagnation-point pressure.

The EDL system will employ a Dacron® supersonic parachute. The required parachute deployment conditions are as follows: dynamic pressure no greater than 703 Pa, Mach number greater than 1.2 and less than 2.3, and time from parachute deployment to 1.5 km AGL (earliest possible ground acquisition by the altimeter) greater than 55 s. This 55-s requirement allows sufficient time, including margin, for parachute stabilization, release of the heatshield, and lander deployment along the 20-m bridle.

The 3σ Pathfinder landing ellipse on the surface of Mars is required to be no larger than 100 × 300 km, centered on the coordinates 19.5°N, 32.8°W. The elevation of the designated landing site is nominally 0.6 km below the Mars reference ellipsoid.

Nominal Entry Trajectory

The nominal trajectory for the Pathfinder entry vehicle has been based on a worst-case entry mass of 603 kg, which corresponds to a ballistic coefficient of 65 kg/m^2 at peak heating (assuming $C_D = 1.68$). The arrival inertial velocity at the atmospheric interface point will depend upon the launch date, but will be within the range of 7.25–7.35 km/s. For design purposes, the maximum entry velocity is used. Note that the arrival velocity increases with later launch dates, so an earlier launch date will result in additional margin. The nominal design entry state is given in Table 1, expressed in the Mars Mean Equator and Prime Meridian of Epoch coordinate

Table 1 Nominal Mars atmospheric entry state: Mars Mean Equator and Prime Meridian of Epoch

Entry date and time (UTC)	7/4/97, 16:46:34
Radius	3522.2 km
Latitude	22.9840°
Longitude	338.9036°
Velocity	7.3509 km/s
Flight-path angle	−14.2 deg
Flight-path azimuth	253.0995 deg

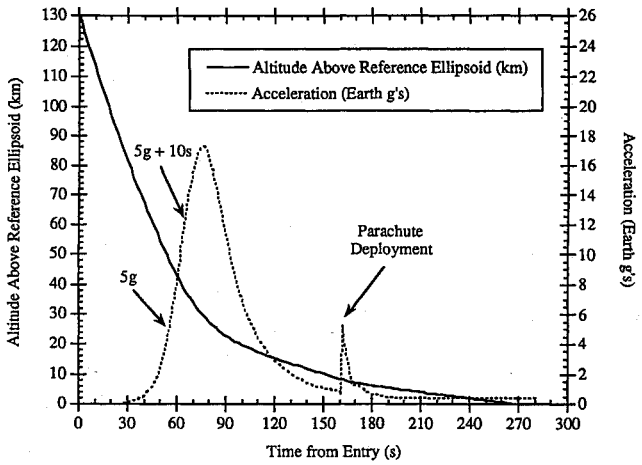

Fig. 3 Altitude and acceleration during entry.

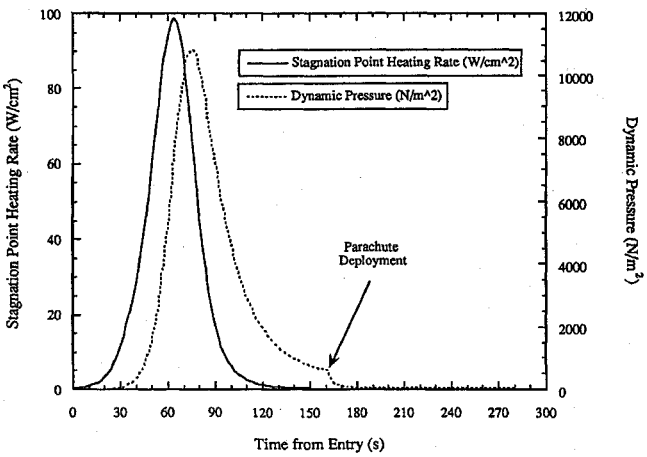

Fig. 4 Heating rate and dynamic pressure during entry.

frame. The nominal entry flight-path angle is −14.2 deg, which provides a 2-deg margin with respect to the −11.2-deg skipout angle, taking into account a ±1-deg navigational uncertainty (3σ).

A plot of altitude and acceleration vs time during entry for the nominal trajectory is shown in Fig. 3. This trajectory reaches a maximum stagnation-point pressure of 21.116 kPa, just prior to reaching the peak cold-wall stagnation-point heating rate of 99 W/cm^2. The maximum acceleration during entry is 17.3 Earth g (169.5 m/s^2). The parachute is deployed at a dynamic pressure of 600 N/m^2, at a Mach number of 2.10. Heating rate and dynamic pressure during entry are shown in Fig. 4. Following the release of the heatshield, the terminal velocity of the system is 58 m/s, at an altitude of 50 m above the assumed ground level. The total integrated stagnation-point heat load during the descent is 3600 J/cm^2.

Throughout the entry portion of the flight, vehicle spin and aerodynamic damping are relied upon to provide vehicle stability about the nominal 0-deg trim total angle of attack. The entry vehicle will enter the atmosphere with a nominal 2-rpm roll rate. A six-DOF aerodynamic assessment has shown that the Mars Pathfinder aeroshell is aerodynamically stable over a large portion of the atmospheric flight.[6,7] However, two low total angle of attack static instabilities (hypersonic) and a low total angle of attack dynamic instability (supersonic) have been identified. These regions of instability, as shown in Fig. 5, cause an increase in vehicle total angle of attack away from the trim state. In each of these flight regimes, the vehicle is aerodynamically stable at higher angles of attack, so that the increase in vehicle total angle of attack is bounded. The nominal attitude profile is characterized by the following: an increase in vehicle total angle of attack just prior to peak heating; flight with a lower total angle of attack, but higher oscillation frequency through peak dynamic pressure; a second increase in vehicle total angle of attack just prior to peak Reynolds number, which is quickly damped; and a final increase in vehicle total angle of attack as parachute deployment is reached.

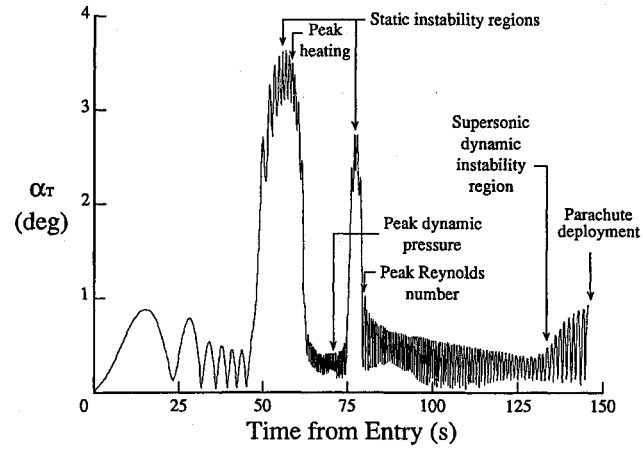

Fig. 5 Nominal six-DOF total angle of attack profile.

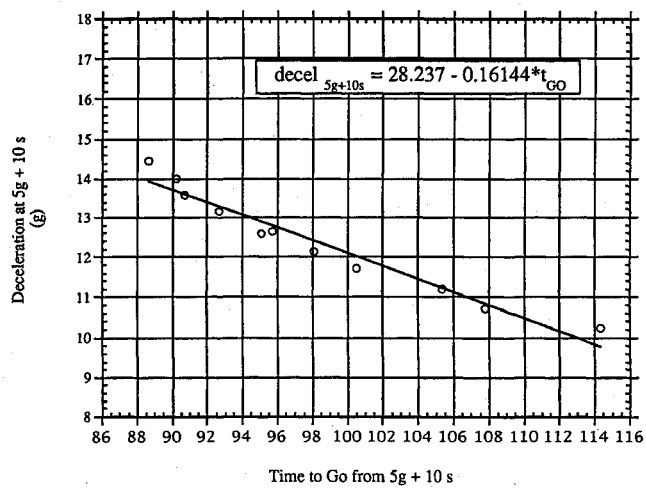

Fig. 6 Linear least-squares fit for parachute deployment.

Parachute Deployment Algorithm

The Mars Pathfinder primary parachute deployment algorithm is based upon accelerometer measurements and a predetermined entry acceleration profile. The algorithm is tuned specifically to the Pathfinder entry trajectory for a ballistic coefficient of 65 kg/m^2 and includes the six-DOF angle of attack variations on vehicle lift and drag. An on-board timer is initiated when the sensed acceleration during atmospheric entry increases to 5 Earth g (49.0 m/s^2; see Fig. 3). Ten seconds after timer initiation, the acceleration is measured once again. Based upon this sensed acceleration at 5 g plus 10 s, a stored curve fit is consulted to determine the time of parachute deployment. The curve fit, shown in Fig. 6, is a linear least-squares approximation to a series of data points derived by propagating six-DOF entry trajectories of various flight-path angles to a targeted dynamic pressure of 600 N/m^2. This target dynamic pressure was determined iteratively, using Monte Carlo simulations to satisfy the 3σ high parachute deployment dynamic pressure requirement of 703 N/m^2, while allowing the parachute to open at a sufficiently high altitude to allow the EDL sequence of events to occur. The Pathfinder parachute deployment algorithm has been implemented

Table 2 Post-TCM-4 covariance matrix

	$B \cdot R$	$B \cdot T$	t_L
$B \cdot R$	8.68487E+01 km^2	−2.98679E+01 km^2	9.47214E − 01 km · s
$B \cdot T$	−2.98679E+01 km^2	5.90933E+01 km^2	−8.51510E − 01 km · s
t_L	9.47214E−01 km · s	−8.51510E−01 km · s	4.52807E − 01 s^2
$S \cdot R$	6.21208E−06 km	−1.85256E−06 km	6.36024E − 08 s
$S \cdot T$	−2.00968E−06 km	4.83299E−06 km	3.90398E − 08 s
C_3	−3.15066E−05 km^3/s^2	5.29953E−06 km^3/s^2	2.47995E − 05 km^2/s
	$S \cdot R$	$S \cdot T$	C_3
$B \cdot R$	6.21208E−06 km	−2.00968E−06 km	−3.15066E − 05 km^3/s^2
$B \cdot T$	−1.85256E−06 km	4.83299E−06 km	5.29953E − 06 km^3/s^2
t_L	6.36024E−08 s	3.90398E−08 s	2.47995E − 05 km^2/s
$S \cdot R$	8.83108E−13 rad^2	−1.35054E−13 rad^2	−2.61029E − 12 km^2/s^2
$S \cdot T$	−1.35054E−13 rad^2	7.92739E−13 rad^2	−5.13206E − 13 km^2/s^2
C_3	−2.61029E−12 km^2/s^2	−5.13206E−13 km^2/s^2	2.11270E − 09 km^4/s^4

in the Monte Carlo simulations. Within the simulations, uncertainties are included for the accelerometer measurements (±4.9 m/s^2, 3σ) and time measurements (±0.25 s, 3σ).

On-board fault protection determines the validity of the accelerometer measurements. If it is determined that the measured accelerations are invalid during the primary opportunity, a backup approach will be implemented. Based on orbit knowledge following the final trajectory correction maneuver (TCM-4), it is possible to specify a fixed time [in terms of coordinated Universal Time (UTC) or Ephemeris Time] at which the parachute can be safely opened. As additional tracking data are received while the spacecraft nears Mars, the navigation estimate of the atmospheric entry time becomes increasingly accurate, and the probability of success of the fixed time approach increases. Monte Carlo results indicate that the fixed time approach provides greater than an 80% likelihood that the parachute will be deployed within the required conditions, based upon tracking data at 5 days prior to entry. In the final day prior to entry, this likelihood increases to over 90%.

Entry-Trajectory Simulation Models

Atmosphere Model

The principal atmosphere model that has been used in the development of the Pathfinder entry trajectory is Version 3.0 of the Mars Global Reference Atmospheric Model (Mars-GRAM).[8] Mars-GRAM includes mean density, temperature, pressure, and wind profiles, and statistical perturbation magnitudes for density variations. The model includes diurnal, seasonal, and positional (i.e., latitude and longitude) variations, as well as optional dust-storm effects. Additional effects, such as solar flux and terrain-influenced atmospheric waves, are also available.

In the June 1994 Mars Pathfinder landing-site selection workshop, the scientific community was in agreement that the Mars-GRAM atmosphere model was the most accurate model available. Since that time, Hubble Space Telescope observations and Earth-based microwave measurements have indicated that the atmosphere of Mars is significantly cooler and has a lower dust content than when it was observed by the Viking Landers. An atmosphere model (which will be referred to as the Clancy model) has been developed that is correlated to the more recent data.[9]

Figure 7 shows the density variation of the Clancy model compared with the Mars-GRAM mean profile, as a function of altitude. Also shown for reference are the Mars-GRAM 3σ low and high density profiles, the COSPAR 3σ low and high density profiles (used by the Viking program), and the Pathfinder model, that is used in the Monte Carlo simulations. Within Mars-GRAM, the computed 1σ density variations with respect to the mean are multiplied by 3 to obtain the 3σ variations shown in Fig. 5. This can result in density variations greater than 100% in the upper altitude region, producing negative density values. For the Pathfinder Monte Carlo simulations, atmospheric density uncertainties twice those computed in Mars-GRAM are used in the region below 75-km altitude (i.e., a Mars-GRAM 6σ density profile would be treated as a 3σ profile in the Monte Carlo analysis). For altitudes above 100 km, where the effect of the atmosphere on the entry trajectory is minor, atmospheric

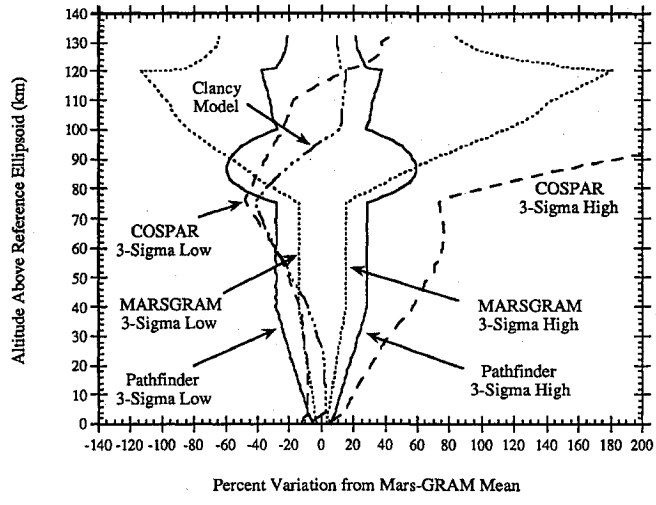

Fig. 7 Mars atmospheric density models compared with Mars-GRAM mean.

density uncertainties one-third as great as those given by the Mars-GRAM 3σ profiles are used. This is done to avoid the possibility of obtaining negative density values. Between 75- and 100-km altitude, the density uncertainty is linearly interpolated between the higher- and low-altitude uncertainty values. As seen in Fig. 7, the Clancy model predicts atmospheric densities below the current Pathfinder 3σ low density profile for altitudes between 45 and 80 km (as does the COSPAR model). The effects of these models on the Pathfinder entry trajectory dispersions are currently being evaluated.

Entry Covariance Matrix

Initial conditions at the atmospheric interface point are generated by randomly sampling a covariance matrix, which is computed using the Jet Propulsion Laboratory's Orbit Determination Program. The 1σ covariance matrix is expressed in terms of B-plane coordinates $B \cdot R, B \cdot T$; the linearized time of flight t_L; $S \cdot R$; $S \cdot T$; and the square of the incoming hyperbolic excess velocity (C_3). The B-plane coordinate system is described fully in Ref. 10. A dispersed initial state is generated by multiplying the 6 × 6 Cholesky factor of the covariance matrix by a randomly generated 6 × 1 vector, and adding the resulting dispersion vector to the nominal 6 × 1 state vector. The elements of the 6 × 1 random vector are generated assuming a normal distribution with zero mean and unit variance. The covariance matrix is produced for the trajectory following TCM-4, and the resulting inertial entry flight-path angles have a 3σ variation of ±1 deg from the nominal value. The covariance matrix that is used in the Monte Carlo simulations is shown in Table 2.

Gravity Field and Reference Ellipsoid

The Monte Carlo simulation employs a simple gravity field with J_2 only, assuming a gravitational parameter for Mars of 42,828.29 km^3/s^2 and a J_2 term of 0.0019628. The Mars reference ellipsoid

Table 3 Entry-body mass properties

Entry mass	603 kg
Center of mass	$X = 0$ m
	$Y = 0$ m
	$Z = 0.818$ m
Inertia properties	$I_{XX} = 196.5272$ kg · m^2
	$I_{YY} = 201.7589$ kg · m^2
	$I_{ZZ} = 248.5768$ kg · m^2
	$I_{XY} = -1.1602$ kg · m^2
	$I_{XZ} = -0.23599$ kg · m^2
	$I_{YX} = -0.57048$ kg · m^2

that is used for altitude determination has equatorial semiaxes of 3394.67 and 3393.21 km and a polar semiaxis of 3376.78 km.

Mass Properties

Worst-case mass properties for the entry vehicle are used. This corresponds to a ballistic coefficient prior to peak heating of 65 kg/m^2. The entry-body mass properties are given in Table 3. The coordinate system for the mass properties, shown in Fig. 1, has its origin located on the centerline of the vehicle, at the top of the cruise-stage/entry-vehicle interface pads. The $+Z$ axis is directed along the spacecraft centerline, toward the tip of the conical aeroshell. The $+Y$ axis is in the direction opposite interface bushing 1, and the $+X$ axis completes the right-handed system.

Integrators

The three- and six-DOF Monte Carlo simulations were developed independently, and employ different numerical integrators. The three-DOF Atmospheric Entry Program (AEP) uses a double-precision, variable-order Adams predictor–corrector method. A standard double-precision, fourth-order Runge–Kutta integration method is applied for the six-DOF Program to Optimize Simulated Trajectories (POST) computations.

Aerodynamics

An aerodynamics database was developed for use in the Monte Carlo analyses based on a combination of computational fluid dynamics calculations and wind-tunnel and ballistic-range test results.[7] Proper estimation of the drag coefficient is required for the three-DOF analysis, whereas the six-DOF simulation requires three force coefficients as well as static and dynamic moment coefficients. In this work, the total angle of attack means the angle between the longitudinal axis of the axisymmetric entry body and the atmosphere-relative velocity vector. Aerodynamic characteristics were obtained for the forebody of the Mars Pathfinder 70-deg sphere–cone aeroshell at numerous trajectory points (from entry interface to Mach 1.5), over a total angle of attack range of 0–11 deg, with the HALIS[11] and the LAURA codes.[12] Base effects on the drag coefficient were calculated by including the afterbody in several of the full-chemistry Navier–Stokes (LAURA) solutions. These computational data were supplemented by Viking test data and compared with the Viking flight data for 11-deg total angle of attack. The complete aerodynamic database is presented in Ref. 7.

The entry-vehicle drag coefficient as a function of total angle of attack and relative velocity is depicted in Fig. 8. The peak aeroshell drag coefficient is 1.71. Three-sigma uncertainty levels for each aerodynamic coefficient were estimated. These subjective estimates were based on computational experience and comparison with similar entry configurations at similar flowfield conditions. For the drag coefficient, an uncertainty of 2% was determined above Mach 10. Below Mach 5, the unsteady base flowfield has a greater influence, and there is less computational experience with the LAURA code. A 3σ uncertainty on the drag coefficient of 10% was used below Mach 5. Between Mach 5 and Mach 10, a linearly interpolated value for drag coefficient variation was used.

Both the computational solutions and the Viking ballistic-range test data identify two low angle of attack static instability regions, at atmosphere-relative velocities of 6.5 and 3.5 km/s. These regions are discussed in detail in Ref. 6. Experimental data produced in support of the Viking program also predict the presence of a low angle of attack dynamic instability region below Mach 2.5. The effect of the three instability regions on the Pathfinder mission is discussed in Ref. 1.

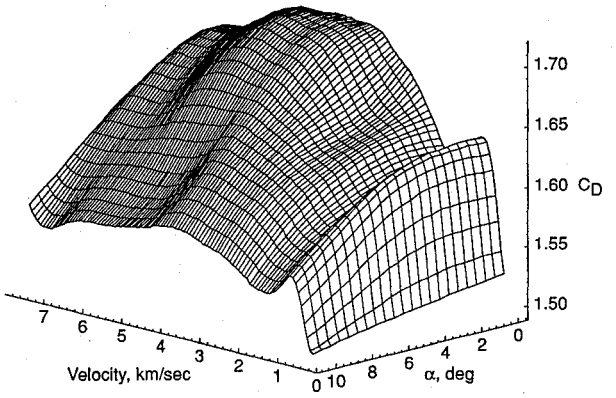

Fig. 8 Pathfinder drag coefficient as a function of angle of attack and velocity.

Cruise-Stage Separation

Based on the current set of Pathfinder mass properties, a statistical cruise-stage separation analysis predicts a 3σ pointing error of 2.68 deg, a 3σ nutation of 4.36 deg, and a 3σ wobble of 1.97 deg at the atmospheric interface point. These predictions translate into a maximum ±9-deg total angle of attack and a maximum total attitude rate of ±1.5 deg/s at the atmospheric interface point. These uncertainties are provided as input to the six-DOF Monte Carlo analysis.

Monte Carlo Simulation and Statistical Analysis

While computationally intensive, the Monte Carlo approach can give insight into the behavior of systems that are too complex to be resolved analytically. Three-DOF (translational) and six-DOF (translational and rotational) Monte Carlo simulations have been developed to obtain statistical information on conditions at critical points during the Pathfinder descent. Because the six-DOF simulation is more complete in its representation of the entry-body aerodynamics, these results are used for verification of EDL system requirements. The three-DOF simulation is useful for modeling the terminal descent phase of the trajectory, following parachute deployment, and, as an independent simulation, the three-DOF simulation provides a useful check of the six-DOF results.

Table 4 contains the variables for the Monte Carlo simulations. The perturbed initial entry state is determined as described in the earlier Entry Covariance Matrix subsection. The atmospheric density profile is determined by two randomly generated scale factors, for the upper (above 100 km) and lower (below 75 km) atmosphere. Between 75 and 100 km, the scale factor is linearly interpolated from the upper and lower altitude scale factors. The scale factors are multiplied by the Mars-GRAM density standard deviation, and the resulting density perturbations are added to the Mars-GRAM mean density profile. While this approach for generating density profiles does not necessarily result in profiles that are physically realizable, it bounds the likely profiles and produces meaningful statistical results when used in a Monte Carlo simulation. The dispersions on event timing and accelerometer measurements shown in Table 4 are applied to the parachute deployment algorithm. The six-DOF Monte Carlo simulation includes additional uncertainties on aerodynamic coefficients, entry-body center of gravity location, and initial attitude and attitude rates.

Results from the three- and six-DOF Monte Carlo simulations are shown in Table 5. For both simulations, 2000 cases were run. Trajectory and attitude conditions are given at critical points during atmospheric entry, in terms of the statistical mean, standard deviation, and 3σ range. Altitudes in Table 5 are given with respect to the Mars reference ellipsoid. Velocity and flight-path angle are given with respect to an atmosphere-relative coordinate frame.

The six-DOF simulation terminates at the time of parachute deployment. The six-DOF conditions at parachute deployment are passed into the three-DOF simulation, so that values can be obtained at the times of heatshield release, bridle deployment, and rocket assisted deceleration (RAD) firing. A complete multibody

Table 4 Monte Carlo simulation variables

Input variable	Nominal	Variation	Distribution
Initial entry state	$r = 3522.2$ km $\gamma = -14.2$ deg	Based upon covariance matrix	Normal
Center of mass offset	815.8 mm axial 0.0 mm radial	± 33 mm (3σ) ± 5 mm (3σ)	Normal
Entry α_T	0.0 deg	9 deg (3σ)	Normal
Entry yaw and pitch rates	0.0 deg/s	1.1 deg/s (3σ)	Normal
Entry roll rate	12.0 deg/s	0.6 deg/s (3σ)	Normal
Atmospheric density	Mars-GRAM mean	Mars-GRAM $\pm 6\sigma$ below 75 km, Mars-GRAM $\pm 1\sigma$ above 100 km, linearly interpolated between 75 and 100 km	Normal
Aerodynamic coefficients	Langley aerodynamics database	See Ref. 1	Normal
Parachute drag coefficient	Viking drag profile	$\pm 13\%$ (3σ)	Normal
Accelerometer error	0.0 m/s^2	± 4.9 m/s^2 (3σ)	Normal
Event timing error	0.0 s	± 0.25 s (3σ)	Normal
Landing site elevation	-0.60 km	± 1.0 km (3σ)	Normal

Table 5 Results of simulations

	Three DOF			Six DOF		
Event	Mean value	Standard deviation	3σ range	Mean value	Standard deviation	3σ range
Peak heating rate, W/cm^2	98.57	2.45	91.21–105.92	98.09	2.65	90.14–106.04
Peak heating α_T, deg	——[a]	——[a]	——[a]	4.88	0.53	3.29–6.47
Peak acceleration, Earth g	17.25	0.97	14.33–20.17	17.27	0.91	14.54–20.00
Max. stagnation-point pressure, kPa	21.101	1.182	17.555–24.647	20.78	1.11	17.45–24.11
Parachute deployment						
Time from entry, s	162.70	9.58	133.97–191.44	162.93	8.81	136.50–189.36
Altitude, km	8.01	0.80	5.63–10.40	7.94	1.16	4.46–11.42
Velocity, km/s	0.386	0.015	0.340–0.431	0.386	0.026	0.308–0.464
γ, deg	−25.83	0.90	−28.53– −23.12	−25.93	1.81	−31.36– −20.50
α_T, deg	——[a]	——[a]	——[a]	1.77	0.76	0.00–4.05
Acceleration, Earth g	——[a]	——[a]	——[a]	0.833	0.044	0.701–0.965
Mach number	1.72	0.07	1.51–1.94	1.72	0.12	1.36–2.08
Dynamic pressure, N/m^2	585.9	35.0	480.87–691.0	586.1	39.1	468.8–703.4
Heatshield release						
Time from entry, s	182.70	9.58	153.97–211.44	182.93	8.81	156.50–209.36
Altitude, km	5.92	0.77	3.60–8.25	5.85	1.13	2.46–9.24
Velocity, km/s	0.110	0.006	0.093–0.127	0.111	0.014	0.070–0.151
γ, deg	−45.65	1.39	−49.83– −41.48	−45.76	2.95	−54.60– −36.91
Acceleration, Earth g	0.729	0.029	0.643–0.815	0.734	0.066	0.537–0.931
Mach number	0.49	0.03	0.41–0.56	0.49	0.06	0.31–0.67
Dynamic pressure, N/m^2	57.1	4.2	44.4–69.7	58.8	12.9	20.1–97.6
Total integrated heating, J/cm^2	3615	89	3348–3881	3602	91	3329–3875
Bridle fully deployed						
Time from entry, s	207.70	9.58	178.97–236.44	207.93	8.81	181.50–234.36
Altitude, km	4.10	0.75	1.86–6.34	4.02	1.09	0.75–7.30
Velocity, km/s	0.074	0.002	0.067–0.082	0.075	0.006	0.057–0.092
γ, deg	−74.69	1.13	−78.09– −71.28	−74.62	2.61	−82.43– −66.80
Acceleration, Earth g	0.396	0.002	0.388–0.403	0.397	0.005	0.381–0.413
Mach number	0.33	0.01	0.30–0.36	0.33	0.03	0.25–0.41
Dynamic pressure, N/m^2	31.0	1.5	26.5–35.4	31.6	4.8	17.3–45.9
Ground acquisition (1500-m AGL)						
Time from chute deploy, s	92.23	11.55	57.57–126.89	90.95	16.82	40.50–141.40
RAD firing						
Time from entry, s	278.00	17.13	226.60–329.41	276.78	20.78	214.43–339.12
Altitude, km	−0.484	0.322	−1.450–0.482	−0.487	0.327	−1.469–0.493
Velocity, km/s	0.058	0.002	0.052–0.063	0.058	0.004	0.045–0.071
γ, deg	−89.72	0.22	−90.00– −89.06	−89.56	0.60	−90.00– −87.74
Acceleration, Earth g	0.398	0.001	0.394–0.403	0.399	0.003	0.389–0.408
Mach number	0.26	0.01	0.24–0.29	0.26	0.02	0.20–0.32
Dynamic pressure, N/m^2	31.2	1.4	26.9–35.5	31.7	4.6	17.9–45.5

[a]Computed in six-DOF simulation only.

(parachute, backshell, and lander) simulation for the terminal descent phase of the entry trajectory is in development at the JPL Mechanical Systems Engineering and Research Division.

In general, there is excellent agreement between the three- and six-DOF simulations on the mean values of the trajectory conditions at the various EDL events. However, it is seen that the standard deviations for the six-DOF results are often larger than those for the three-DOF data. This greater variation is due to the initial attitude errors and the aerodynamic effects allowed for in the six-DOF simulation, namely, a variation in the drag coefficient due to a changing total angle of attack, as well as lift effects.

A histogram of the total angle of attack at peak heating (computed in the six-DOF simulation) is shown in Fig. 9. This information was necessary for the aeroshell design. Figure 10 shows a scatter plot of the six-DOF altitude and dynamic pressure at the time of parachute deployment. It is seen that several cases had parachute deployment

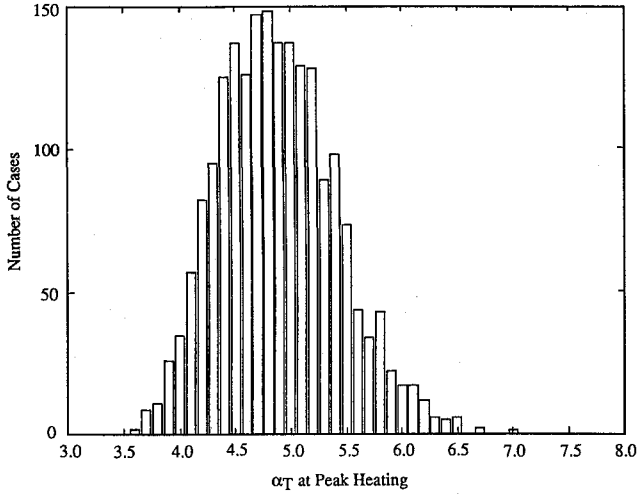

Fig. 9 Six-DOF histogram for total angle of attack at peak heating.

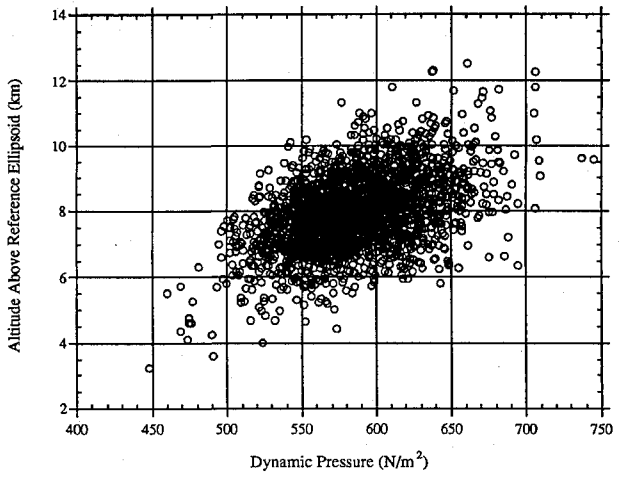

Fig. 10 Six-DOF altitude and dynamic pressure at parachute deployment.

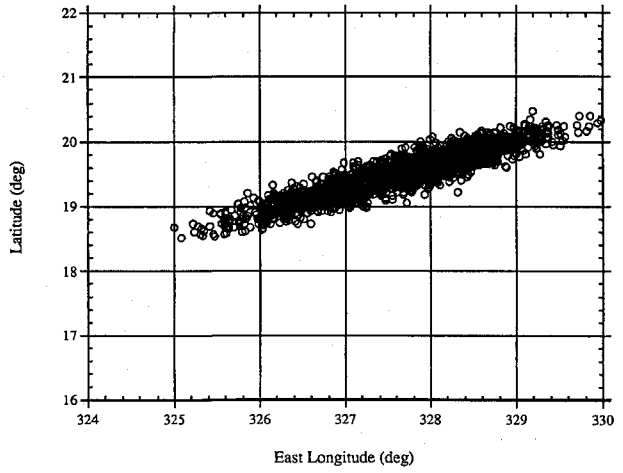

Fig. 11 Three-DOF landing ellipse.

dynamic pressures that exceeded the parachute limit of 703 Pa; however, the 3σ range of parachute deployment conditions is within the requirements. The three-DOF landing ellipse on the Mars surface is shown in Fig. 11. The 3σ landing ellipse measures 45×299 km, which is within the required 100×300 km ellipse. The Monte Carlo simulation results indicate that the required conditions at parachute deployment are met by the 3σ range of trajectories. The range of total integrated heating and the dynamic pressures at heatshield release are within the limits of the aeroshell design. The EDL system requirement of 55 s from parachute deployment to 1500-m altitude AGL is met in 2.1σ (95%) of the six-DOF trajectories. This is an acceptable risk level to the Pathfinder Project, as recent design improvements in the bridle subsystem have increased the margin in the terminal descent timeline.

Conclusion

Design of the Pathfinder entry trajectory and identification of the likely trajectory dispersions during critical events have been essential for the development of the various EDL subsystems. Monte Carlo simulations have been instrumental in quantifying the statistical uncertainties associated with trajectory and attitude conditions during the atmospheric entry. In general, the six-DOF simulation results are used to determine the 3σ bounds on trajectory and attitude conditions during entry, up to the time of parachute deployment. The three-DOF simulation is useful for preliminary trade studies and for simulation of the terminal descent (after parachute deployment). In addition, the three-DOF simulation provides an independent check of the six-DOF results.

The nominal Pathfinder entry trajectory design currently meets all EDL requirements with a significant amount of margin, providing a high level of confidence that Pathfinder's five minutes of flight through the Mars atmosphere will result in a successful landing.

Acknowledgments

The work described in this paper was carried out by the Jet Propulsion Laboratory, California Institute of Technology, and NASA Langley Research Center, under a contract with NASA. The authors would like to acknowledge the contributions of several individuals to this work. Richard Cook was responsible for the Mars Pathfinder interplanetary trajectory design and the early atmospheric entry trajectory design. Gurkirpal Singh contributed to the design of the parachute deployment algorithm. Pieter Kallemeyn provided the entry covariance matrix. Vince Pollmeier developed the early Monte Carlo simulation capability. Walt Engelund, Peter Gnoffo, Bob Mitcheltree, and James Weilmuenster developed the entry-body aerodynamics database.

References

[1]Braun, R. D., Powell, R. W., Engelund, W. C., Gnoffo, P. A., Weilmuenster, K. J., and Mitcheltree, R. A., "Mars Pathfinder Six-Degree-of-Freedom Entry Analysis," *Journal of Spacecraft and Rockets*, Vol. 32, No. 6, 1995, pp. 993–1000.

[2]Congdon, W. M., "Ablation Model Validation and Analytical Sensitivity Study for the Mars Pathfinder Heat Shield," AIAA Paper 95-2129, June 1995.

[3]Cook, R. A., and McNamee, J. B., "Mission Design for the Mars Environmental Survey," American Astronomical Society, Paper 93-563, Aug. 1993.

[4]Seiff, A., "Mars Atmospheric Winds Indicated by Motion of the Viking Landers During Parachute Descent," *Journal of Geophysical Research*, Vol. 98, No. E4, 1993, pp. 7461–7474.

[5]Golombek, M. P., Edgett, K. S., and Rice, J. W., Jr. (eds.), "Mars Pathfinder Landing Site Workshop II: Characteristics of the Ares Vallis Region and Field Trips to the Channeled Scabland, Washington," Lunar and Planetary Inst., TR 95-01, Pt. 1, Houston, TX, 1995.

[6]Gnoffo, P. A., Weilmuenster, K. J., Braun, R. D., and Cruz, C. I., "Effect of Sonic Line Transition on Aerothermodynamics of the MESUR Pathfinder Probe," AIAA Paper 95-1825, June 1995.

[7]Engelund, W. C., Gnoffo, P. A., Cruz, C. I., Braun, R. D., and Weilmuenster, K. J., "Aerodynamic Characteristics of the Mars Pathfinder Atmospheric Entry Configuration," NASA TM (in preparation).

[8]Justus, C. G., and Chimonas, G., "The Mars Global Reference Atmospheric Model (Mars-GRAM)," TR, Georgia Tech Project G-35-685, prepared for NASA Marshall Space Flight Center under Grant NAG8-078, July 1989.

[9]Clancy, R. T., Lee, S., Gladstone, G., Mcmillan, W., and Rousch, T., "A New Model of Mars Atmospheric Dust Based upon Analysis of Ultraviolet Through Infrared Observations from Mariner-9, Viking, and Phobos," *Journal of Geophysical Research*, Vol. 100, 1995, pp. 5251–5263.

[10]Taylor, A. H., Ionasescu, R., and Vaughan, R. M., "A First Look at Orbit Determination for the Cassini Mission," American Astronomical Society, Paper 93-603, Aug. 1993.

[11]Weilmuenster, K. J, and Hamilton, H. H., II, "Computed and Experimental Surface Pressure and Heating on 70-deg Sphere Cones," *Journal of Spacecraft and Rockets*, Vol. 24, No. 5, 1987, pp. 385–393.

[12]Gnoffo, P. A., "Upwind-Biased, Point-Implicit Relaxation Strategies for Viscous, Hypersonic Flows," AIAA Paper 89-1972, June 1989.

F. H. Lutze
Associate Editor